Soft Matter

PAPER

View Article Online
View Journal

Physicochemical characterization of partially hydrolyzed poly(vinyl acetate)–borate aqueous dispersions†

Cite this: DOI: 10.1039/c4sm00355a

E. Carretti, C. Matarrese, E. Fratini, P. Baglioni and L. Dei*

The dynamic and structural properties of Highly Viscous Polymeric Dispersions (HVPDs), constituted of polyvinyl alcohol obtained from the 75% hydrolysis (75PVA) of polyvinlyl acetate (PVAc) cross-linked with borate ions, were studied as a function of the 75PVA concentration at a constant ratio between the OH groups and the borate ions ($OH/B(OH)_4^-$). The threshold 75PVA concentration C^* necessary for the formation of the three-dimensional network was determined by flow rheology. The oscillating rheology measurements were performed in the linear viscoelastic region; the relaxation spectra calculated from the frequency sweep curves showed only one peak whose width increased upon increasing the 75PVA concentration due to the broadening of the relaxation modes. The dependence of the mean relaxation time τ_H upon the concentration of 75PVA followed a power law expression ($\tau_H \sim C^x$ with $x = 1.9$) indicating that τ_H referred to a sticky reptation mechanism and that water was a good solvent for 75PVA as confirmed also by small angle X-rays scattering (SAXS) investigation. The HVPDs were used for the removal of grime layers from the surface of Carlo Carrà (1881–1966) paints decorating the walls of the *Palazzo di Giustizia* in Milan, Italy.

Received 14th February 2014
Accepted 31st March 2014

DOI: 10.1039/c4sm00355a

www.rsc.org/softmatter

Introduction

Poly(vinyl alcohol) (PVA), synthesized for the first time by Herrmann and Haehnel in 1924 through the hydrolysis of poly(vinyl acetate) (PVAc), due to its low price, biodegradability, biocompatibility, and solubility in water, is largely used in cosmetics, fibers, packaging, adhesives, textile industries and for the set up of innovative pharmaceutical and biomedical materials.[1–9]

Polyvinyl alcohols are commercially available in a broad range of hydrolysis degrees and molecular weights making it possible to significantly modulate their properties to optimize their performances for specific applications. This versatility has sparked interest on the study of the physico-chemical properties of aqueous solutions of *x*PVA,[10] mainly on the study of the properties related to the polymer concentration,[11,12] on the rheological properties,[13] and on the effect of different cross-linking agents that allow the formation of chemical (*i.e.* using glutaraldehyde as a cross-linker) or physical gels (from hydrogen bonds involving the hydroxyl groups).[14] An interesting property of *x*PVA aqueous solution is the formation of gel-like systems as a consequence of complexation or reaction with ions such as borate, vanadate or antimonite with the side-chain hydroxyl groups.[15,16] In particular, aqueous solutions of PVA are known to form thermally-reversible high-viscous polymeric dispersions (HVPDs) in the presence of borate ions. The cross-links, made through interchain esterification reactions between pairs of vicinal diols,[17] are dynamic because ester formation is reversible and a steady-state concentration of them is established under isothermal conditions.[16] The conformations of the polymer chains in these HVPDs depend on a balance among electrostatic repulsions, polymer-chain excluded volume, intra- and inter-molecular cross-linking reactions between PVA chains and borate ions, and charge-shielding effects.[18–22]

The PVA–borate HVPDs have been extensively studied in the last decades by dynamic and static light scattering,[21] dynamic viscoelastic measurements,[23] X-ray analysis,[24] and differential scanning calorimetry,[25] as well as by SANS and NMR.[16] From these studies the structure and properties of the PVA–borate HVPDs have been found to depend on the PVA and borate concentrations, temperature, length (average molecular weight) of the PVA chains, and the pH of the aqueous region; depending upon these factors, the HVPDs can be very sticky or quite fluid.[26] In spite of several papers about the structural and mechanical properties of aqueous PVA–borate HVPDs, only a few studies were devoted to the study of the properties of PVAc with lower hydrolysis degrees cross-linked with borate. The possible modulation of their mechanical behavior induced the exploration of their use in the removal of extraneous materials from surfaces of works of art.[27] In the past few years, some studies

Department of Chemistry & CSGI Consortium, University of Florence, via della Lastruccia, 3 – 50019 Sesto Fiorentino, Florence, Italy. E-mail: carretti@csgi.unifi.it; matarrese@csgi.unifi.it; fratini@csgi.unifi.it; baglioni@csgi.unifi.it; dei@csgi.unifi.it

† Electronic supplementary information (ESI) available: Additional rheological data. See DOI: 10.1039/c4sm00355a

dealt with the use of peelable aqueous highly viscous systems[24,28] as innovative tools for cleaning painted and decorative surfaces. For cleaning purposes[29] HVPD should be sufficiently soft to have a good contact with the surface to be treated and its elasticity and viscosity should be sufficiently high to maintain its ability to be easily removed from the surface after cleaning.

In the present paper the structural, mechanical and calorimetric properties of these aqueous viscoelastic dispersions of 75PVA and borate as the cross-linker are presented while maintaining a constant molar ratio between the OH groups and borax. The systems were analyzed by a detailed rheology investigation (in particular, trends between the viscoelastic parameters like the storage modulus (G') and loss modulus (G'') and HVPD compositions). The free water indices (FWI) were determined from differential scanning calorimetry (DSC) measurements and their structural properties were established through small angle X-ray scattering (SAXS) measurements. Some application tests on wall paintings were also reported to assess their possible use in the field of works of art conservation.

Experimental section

75% hydrolyzed poly(vinyl acetate)s (75PVAs), as the random copolymer, was supplied by Kuraray Co., Ltd. It was copiously washed with ice-cold water and dried under vacuum in order to eliminate by-products and residual free acetate. Sodium tetraborate decahydrate (>99.5%, Fluka) was used as received. Water was purified by a Millipore Elix3 apparatus ($R \geq 15$ MΩ cm).

The molecular weight (M) distribution of 75PVA was obtained by means of a Size-Exclusion Chromatography (SEC) apparatus equipped with a column calibration based on dextran standards. The mobile phase was aqueous phosphate-buffered saline (PBS). The molecular weight distribution was obtained by linearly fitting the log M *vs.* elution volume and then generating the M-value using the Empower software from Waters. Analyses were performed using 2 TSKGM PWXL columns (in series) from Tosoh Biosciences and a Waters SEC-LS chromatograph consisting of a Waters Alliance 2690 (solvent delivery and autoinjector) component, a temperature-controlled column compartment, and a Waters 410 differential refractive index detector. The M_w-value determined in this way of 75PVA was 7300.

For the preparation of the HVPDs the polymer was placed in a vial and was dissolved in water by heating under stirring at 85 °C for 2 h. Then, an aliquot of an aqueous 4 wt% borax solution was added drop-wise by stirring (vortex apparatus). The sample became rigid after a few minutes. Mechanical equilibration of all the investigated samples was monitored by means of rheology. Frequency sweeps (*vide infra* for the measurement set up) were carried out 1, 2, 5 and 10 hours after the sample preparation. It was observed that after 2 hours the trend of both the elastic (G') and the loss (G'') moduli remained constant. On the other hand, the chemical equilibrium detected by the invariance of pH was anticipated, since pH remained equal to 7.30 ± 0.20 1 hour after the sample preparation. pH measurements were performed with a digital pH-meter CrisonBasic 20.

All the characterization studies were carried out 24 h after sample preparation to ensure the reaching of equilibrium of the HVPDs. The ratio between the amount of polymer hydroxyl groups and the borate ions ($OH/B(OH)_4^-$) was kept equal to 20.4 : 1 throughout.

For the falling drop studies,[30] a 0.5 g portion of each HVPD, prepared as described above, was sealed in a glass tube and cooled to 5 °C. Then, the tube was inverted and placed in a water bath at 0 °C; the temperature of the bath was raised by 2 °C min^{-1}. The temperature ranges over which each HVPD first showed signs of flow and fell completely were recorded. The falling drop tests normally give the sol–gel transition, whereas in the case of HVPDs the method was used to establish the temperature at which the HVPD's network starts to loose strength (T_{ls}). Before the tests, all the glass tubes were washed with piranha solution and demineralised water.

SAXS measurements were carried out with a HECUS S3-MICRO camera (Kratky-type) equipped with a position-sensitive detector (OED 50M) containing 1024 channels of width 54 μm. Cu Kα radiation ($\lambda = 1.542$ Å) was provided by an ultra-brilliant point micro-focus X-ray source (GENIX-Fox 3D, Xenocs, Grenoble), operating at a maximum power of 50 W (50 kV and 1 mA). The sample-to-detector distance was 269 mm. The space between the sample and the detector was kept under vacuum during the measurements to minimize scattering from the air. The Kratky camera was calibrated in the small angle region using silver behenate ($d = 58.34$ Å).[31] Scattering curves were obtained in the q-range between 0.01 and 0.54 $Å^{-1}$, assuming that $q = 4\pi/\lambda \sin\theta$, where 2θ is the scattering angle. Gel samples were placed into 1 mm demountable cells having Mylar films as windows. Liquid samples were filled into a 1 mm borosilicate Mark-tube (Hilgenberg GmbH, Germany) using a syringe. The borosilicate capillaries were sealed to avoid solvent evaporation. The temperature was maintained at 25 ± 0.1 °C by a Peltier controller. All scattering curves were corrected for the empty cell contribution considering the relative transmission factor.

Oscillatory shear measurements were carried out on a Paar Physica UDS200 rheometer at 25 ± 0.1 °C (Peltier temperature control system) using a cone-plate geometry (25 mm diameter and 1° cone angle). The minimum gap between the plates at the zero radial position was 0.5 mm. The cone was lowered up to the measuring position in the z axis force controlled mode; the maximum squeezing force was 3.0 N. After being loaded, the samples were allowed to equilibrate for 30 min at 25 °C prior to start of the experiments. Frequency sweep measurements were carried out within the linear viscoelastic range (4% strain), determined by means of an amplitude sweep test. The storage and loss moduli (G' and G'', respectively) were measured over the frequency range of 0.01 to 100 Hz. The intrinsic viscosity, η_0, values were deduced from the plateau of the flow curves in the low Newtonian region (low-shear-rate regime). This value was plotted as a function of the polymer concentration in order to determine the threshold 75PVA concentrations C^* above which the drastic increase of the η_0 value indicates the formation of

the extended 3D polymer networks at different ($OH/B(OH)_4^-$) ratios (see Fig. S1†). In order to minimise the handling of the HVPDs, immediately after the addition of the borax solution, the vials were turned upside down to favour the accumulation of the sample on the cap side. Then, all the HVPDs were easily directly transferred onto the measurement plate.

DSC measurements were performed with a Q1000TA Instruments apparatus. The samples, sealed in aluminum pans, were equilibrated at 25 °C, cooled to −90 °C at a cooling rate of 5 °C min^{-1}, kept at −90 °C for 8 min, and then heated to 30 °C at 5 °C min^{-1}, under a 50 mL min^{-1} stream of nitrogen. An empty sealed aluminum pan was used as the reference. For each system, three different samples were prepared and scanned. The enthalpy of fusion of the water was calculated by integrating the heat flow curves. The Free Water Index (FWI), a parameter that represents the percent of free and freezing bound water contained in the samples, was calculated using the following formula:[32]

$$\mathrm{FWI} = \Delta H_{\mathrm{samp}}/\Delta H_{\mathrm{purewater}} \times 100 \quad (1)$$

where ΔH_{samp} is the enthalpy change due to the fusion of the ice contained in the HVPD sample (J g_{water}^{-1}), experimentally determined from the DSC curve; $\Delta H_{\mathrm{freewater}}$ (=333.6 J g^{-1}) is the theoretical value of the specific fusion enthalpy of pure ice at 0 °C.

The HVPD was applied onto the surface of a wall painting by Carlo Carrà 48 hours after its preparation. It was applied directly onto the wall painting surface by means of a spatula and left there for about 5 minutes. The HVPD was peeled from the surface by means of a pincer, without adding any additional liquid component to the remaining polymeric dispersion or on the painting surface after the peeling process. The procedure was repeated twice.

Results and discussion

The falling drop test[33,34] indicated that the T_{ls} of the investigated HVPDs significantly increases upon increasing the 75PVA concentration (Fig. 1A), while the effect of the cross-linker concentration was much less pronounced. The data indicated that the T_{ls} was mainly determined by the number of the hydroxyl groups that are the only ones able to form cross-linking. As indicated by Kanaya *et al.*[35] and by Kjoniksen *et al.*,[36] this behaviour can be interpreted considering that the driving factor for the HVPD formation is the entanglement between polymer chains rather than the borax-modulated cross-linking (Fig. 1B).

The threshold 75PVA concentrations (indicated as C^*) necessary for the formation of an extended three-dimensional network were determined rheologically from the trends of the changes in the zero shear viscosity η_0 as a function of the polymer concentrations: the amounts of both 75PVA and borax were varied incrementally while keeping the ($OH/B(OH)_4^-$) ratio constantly equal to 20.4. The obtained C^* value is 3.0. Furthermore, Fig. S1† indicated that upon increasing the ($OH/B(OH)_4^-$) ratio an increase of the C^* value is observed.

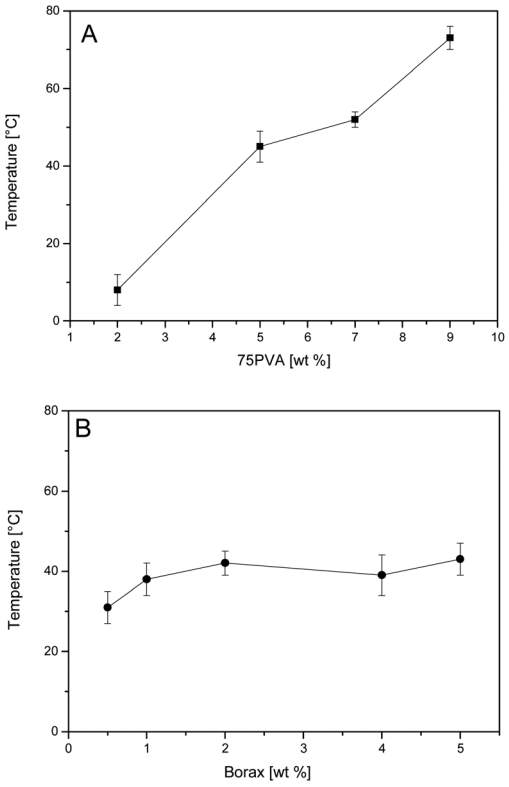

Fig. 1 (A) Variation of the T_{ls} for HVPDs maintaining constant the molar ratio between the –OH groups and $B(OH)_4^-$ ions equal to 20.4; (B) T_{ls} of HVPDs containing 5 wt% of 75PVA. Bars indicate the melting ranges.

Small angle X-ray scattering (SAXS) experiments were conducted to investigate the polymer structure at the nanometer level and to visualize the changes imposed by the presence of borax. Fig. 2 shows the SAXS intensity distribution in the case of 75PVA (see panel A) and 75PVA–borax (panel B) systems from 5 to 12 wt% polymer. All the SAXS curves were modeled according to a functional form[37] that can be interpreted as a generalized version of the Debye–Bueche (DB) approach.[28] The generalized DB model in its original form presents a low-q clustering and high-q solvation contribution plus a flat background, and it has been used to fit small angle neutron scattering curves obtained in the case of both neutral and charged polymeric solutions consisting of synthetic and biological macromolecules.[37] In our case, the low-q clustering term is omitted because no intensity increase was evidenced in the low-q region of the SAXS curves (see both panels of Fig. 2). A previous SANS investigation confirms that the clusters in similar systems are evident only below 0.01 $Å^{-1}$.[16] For this reason, the SAXS curves were modeled according to a solvation term plus a flat background (eqn (2)):

$$I(q) = \frac{I_0}{[I + (|q - q_0|\xi)^m]} + \mathrm{bkg} \quad (2)$$

where I_0 is the scattering intensity at $q = 0$, q_0 is the peak position, ξ is the correlation length which corresponds in a semi-diluted solution to the average distance between neighboring entanglement points,[38] m is the Porod exponent

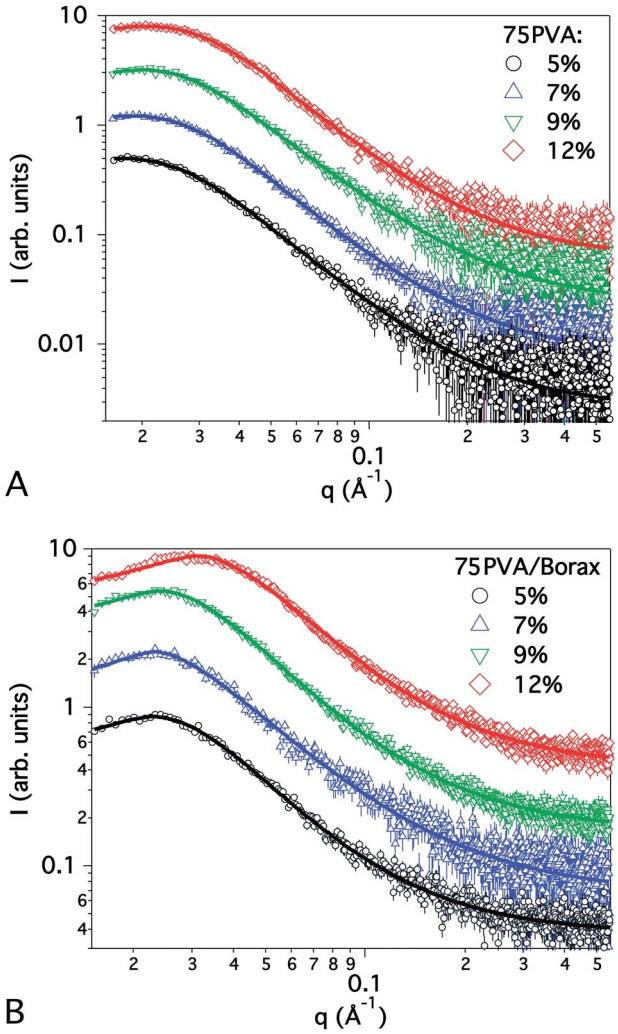

Fig. 2 Double-logarithmic representation of the SAXS intensity distribution for: (A) 75PVA and (B) 75PVA–borax dispersions. The solid lines are the best fits to the scattering points according to eqn (2). The curves are offset vertically by an arbitrary factor to avoid overlap.

Table 1 Parameters associated with the best fits to the SAXS curves of the 75PVA (column A) and 75PVA–borax systems (column B). The (OH/$B(OH)_4^-$) ratio was kept equal to 20.4 : 1 for all the investigated samples

	75PVA			
A	5%	7%	9%	12%
I_0	4.96 ± 0.05	6.02 ± 0.04	5.25 ± 0.07	7.19 ± 0.06
ξ (Å)	55.1 ± 0.04	55.0 ± 0.05	50.7 ± 0.04	49.3 ± 0.04
q_0 (Å^{-1})	0.0168 ± 0.07	0.0188 ± 0.07	0.0189 ± 0.06	0.0208 ± 0.04
M	2.02 ± 0.08	1.98 ± 0.07	1.97 ± 0.08	1.96 ± 0.06
Bkg	0.0268 ± 0.02	0.0396 ± 0.02	0.0487 ± 0.03	0.0572 ± 0.03
	75PVA–borax			
B	5%	7%	9%	12%
I_0	3.34 ± 0.08	5.53 ± 0.02	6.56 ± 0.03	6.14 ± 0.06
ξ (Å)	51.8 ± 0.03	51.1 ± 0.07	50.5 ± 0.06	39.0 ± 0.05
q_0 (Å^{-1})	0.0231 ± 0.08	0.0227 ± 0.09	0.0241 ± 0.04	0.0312 ± 0.03
M	1.69 ± 0.06	1.67 ± 0.06	1.67 ± 0.05	1.64 ± 0.03
Bkg	0.150 ± 0.02	0.157 ± 0.03	0.210 ± 0.05	0.300 ± 0.04

associated with the solvation term and bkg is a q-independent instrumental background term. All these parameters were allowed to vary during the least-square fitting procedure.

Table 1 lists the parameters according to the best fits of the SAXS curves in Fig. 2. While for 75PVA concentrations between 5 wt% and 7 wt% ξ remains constant, a further increase of the amount of the polymer in its dispersions decreased the correlation length from 55.1 to 49.3 nm. The presence of a finite q_0 can be questionable in this 75PVA series because this polymer is expected to be uncharged. However, it must be noted that the q_0 values are very close to the lowest q accessed by the SAXS experiment and, moreover, the curves could also be fitted by constraining q_0 to zero with only a very small increase of the overall χ^2. This result clearly indicated that the charge present on the 75PVA polymer (perhaps as a result of its partial hydrolysis during sample preparation or storage) is almost negligible. q_0 shifted slightly towards high-q as a consequence of increase in the concentration. The average distance between the charges, estimated as $2\pi/q_0$, varied from 37 to 30 nm as the concentration was raised from 5 to 12 wt%. The parameter m has a constant value of 2, corresponding to a Gaussian coil conformation arising from monomer-solvent and monomer–monomer interactions being equal in strength. In the systems in which borax was present, similar considerations hold. However, the correlation lengths decreased by 0.5–1 nm in all cases as a consequence of the cross-links made by the borate ions. The inclusion of these ions in the polymeric network rendered the chains negatively charged, and the interaction peak became more evident and shifted to higher q-values. The associated average distances $2\pi/q_0$ decrease to 27.5–20.1 nm (following the shifts to higher q values imposed on the more concentrated dispersions). In the 75PVA–borax series, the Porod exponent m passed from 2 to about 1.67 as a consequence of the borax addition, which changed the complexity of the network topology and, more importantly, increased the solvent–polymer compatibility. A value of 5/3 (=1.67) describes the behavior of a polymer coil in a 'good' solvent (*i.e.*, when the monomer–solvent interaction is more favorable than monomer–monomer interaction).[36]

In order to understand the effect of the polymer concentration on the mechanical properties of the 75PVA HVPDs and to obtain information about their relaxation dynamics, oscillatory frequency sweep tests were carried out in the linear viscoelastic regime in order to obtain the dependence of the complex moduli G' and G'' on the frequency of the applied shear perturbation. As the 75PVA concentration was increased, the decrease of tan δ indicated enhanced elasticity (see Fig. S2†) due to the increased number of interchain interactions and entanglements between the 75PVA molecules resulting from the decreased chain flexibility and increased molecular size.

As shown in Fig. 3, the 75PVA–borax systems showed a behavior typical of viscoelastic polymeric dispersions; two different regimes can be individuated: for $\omega > \omega_c$ (ω_c is the

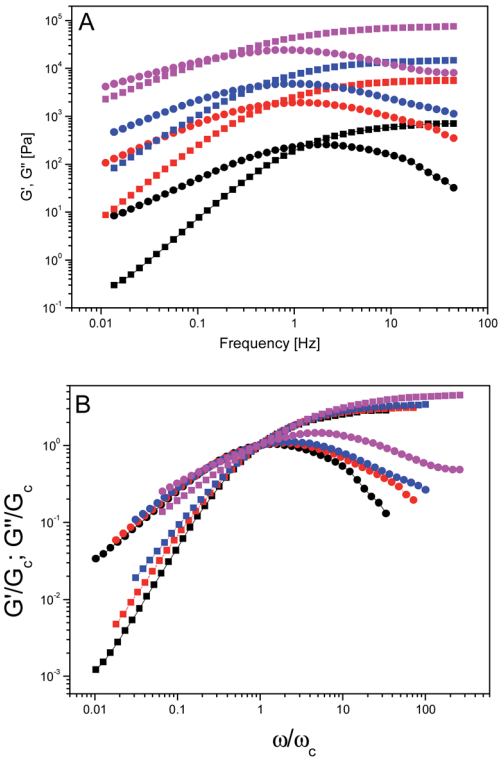

Fig. 3 (A) Frequency sweep curves at 5 (black), 7 (red), 9 (blue) and 12 (purple) wt% 75PVA concentration. Squared symbols indicate the elastic modulus G', circles indicate the loss modulus G''. (B) Normalized mechanical spectra at 2 (black), 5 (red), 7 (blue) and 9 (purple) wt% 75PVA concentrations. Closed symbols indicate the G'/G_c ratio and open symbols indicate the l G''/G_c ratio. G_c and ω_c are the crossover modulus and the crossover frequency respectively.

crossover frequency between the G' and G'' curves) $G' > G''$, indicating a predominantly elastic behavior; for $\omega < \omega_c$ the viscous character prevails ($G' < G''$).

The value of the intrinsic elastic modulus G^0, given by the asymptote of G' curves of the HVPDs, is correlated with the density of the borate-modulated cross-linking (ρ_e) between the 75PVA chains (eqn (3)):

$$G^0 = \rho_e k_B T \quad (3)$$

where k_B is the Boltzmann constant and T is the temperature (K).[39] The increased ρ_e, upon increasing the 75PVA content (Fig. 4), indicated an increase of the complexity of the HVPD structures and an increase of the strength of the 3D network confirming that the driving factor for the formation of the 3D network is the number of OH groups available for the formation of covalent cross-links.

Normalized frequency sweeps are reported in Fig. 3B and indicate that increasing 75PVA and borax concentrations had little effect on the rheological behavior of the HVPDs: the normalized curves overlapped, indicating that, even if the global time scale of the relaxation phenomena slightly changes, the mechanism was almost the same at all concentrations.

Since the dynamic of the 75PVA based HVPDs cannot be described by a single-element Maxwell model (see Fig. S3†),

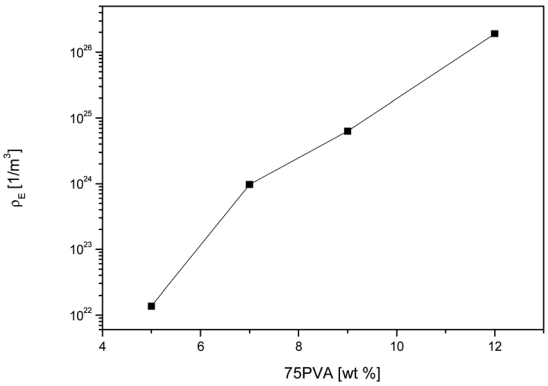

Fig. 4 Effect of the 75PVA concentration on the density of the borate-modulated cross-linking ρ_e on the HVPDs.

both G' and G'' were used to calculate the time-weighted relaxation spectrum $H(\tau)$.[40] In Fig. 5 the $H(\tau)$ spectra are normalized with respect to the zero shear viscosity in order to compare them on similar scales. All the spectra showed only one peak, confirming that the main relaxation mechanism was unchanged upon increasing the 75PVA concentration. However, the observed increase in the width of the spectra indicated that additional modes of relaxation, resulting from increasing entanglements among the polymer chains (*i.e.*, enhancement of polymer–polymer interactions), were operating.

Fig. 6 shows a nearly quadratic dependence of the mean relaxation time τ_H, given by the peak of the relaxation spectra, on the 75PVA concentrations (*i.e.*, $\tau_H \sim C^a$, in the linearised form $\log(\tau_H) = a \log C + b$. The slope a of the plot $\log(\tau_H)$ *vs.* $\log C$ is equal to 1.9). In order to identify the main relaxation mechanism $G(t)$, the trend of the stress relaxation modulus has been investigated. The Doi–Edwards model (eqn (4))[41] for a pure reptation process indicates that $G(t)$ is given by:

$$G(t) = \frac{8}{\pi^2} G^0 \sum_{\text{oddk}} \frac{1}{k^2} \exp\left(-\frac{k^2}{\tau_{\text{rep}}}\right) \quad (4)$$

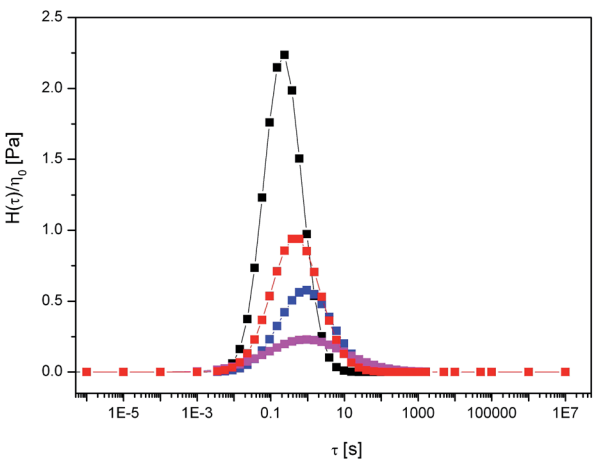

Fig. 5 η_0 normalised stress relaxation spectra ($H(\tau)$) at 5 (black), 7 (red), 9 (blue) and 12 (purple) wt% 75PVA concentration.

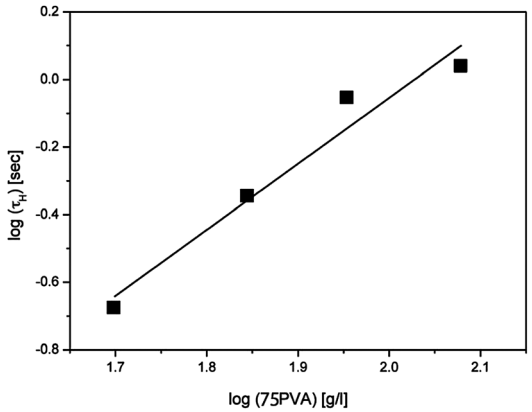

Fig. 6 Effect of the concentration of 75PVA on the mean relaxation times (τ_H) of their HVPDs.

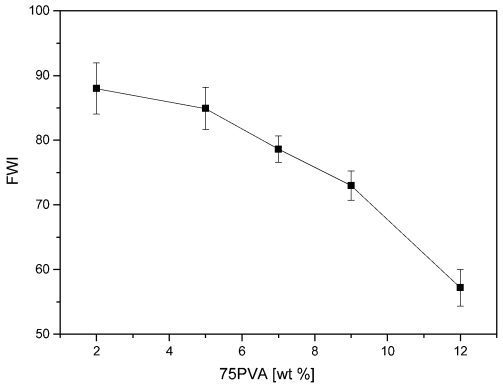

Fig. 7 FWI values of the HVPDs as a function of the 75PVA concentration. The ($OH/B(OH)_4^-$) ratio was kept equal to 20 : 1 for all the investigated samples.

where G^0 is the asymptote of the G' curve and τ_{rep} was taken as the mean relaxation time τ_H of Fig. 5. The comparison between the experimental trend of the stress relaxation modulus and the Doi–Edwards equation indicated that the 75PVA based HVPDs did not relax following a pure reptation mechanism (Fig. S4†). This was probably due to the interchain interactions that slowdown the relaxation process. Rubinstein and Semenov[42] studied the dynamic of entangled solution of associating polymers and demonstrated that their dynamic in good solvents is controlled by the associating groups (stickers). They explained this behaviour in terms of sticky reptation. The corresponding reptation time strongly depends upon the concentration as follows: $\tau_{rep} \sim C_a$, ranging from 1.44 to 4.5 as a function of the length of the strands between 'sticking points'. Our data supported all the HVPDs investigated:

- water is a good solvent as demonstrated also by SAXS data;
- the mean relaxation process is controlled by a sticky reptation mechanism.

In order to estimate the level of interaction of water with the 75PVA–borax network, and relate it to the elastic properties of the polymeric dispersions, the Free Water Index (FWI) was determined from DSC measurements.[18,43]

As seen in Fig. 7, for 75PVA concentrations between 2 wt% and 5 wt%, the FWI value is almost constant. By further increasing the polymer concentration, the percent of non-frozen, bound water at temperatures below 0 °C (*i.e.*, water that interacts strongly with the polymer chains and borate ions) strongly increases up to the 45% for a concentration equal to 12 wt%.

Previous tests carried out on different surfaces[26,44] demonstrated that PVA–borate hydro HVPDs are effective low impact cleaning agents for delicate surfaces of artistical and historical interest. From the applicative point of view, their peculiarities are mainly the gradualness of the cleaning action (that makes these HVPDs suitable for delicate and precious surfaces) and their ease of removal that can be achieved simply by a peeling action, without leaving onto the treated surface any detectable residue. Both these features are strictly related to the rheological properties of the HVPDs. In a previous paper,[29] we proposed a direct correlation between these parameters and the efficacy of the HVPDs in terms of cleaning ability and ease of removal. In particular, we showed that a value of $G^0 > 400$ Pa (G^0 corresponds to the intrinsic elastic modulus given by the asymptotic value of the G' curve, see Fig. 3A) allows the peeling of the cleaning system from the treated surface by a onestep not invasive mechanical action realized by tweezers; all the investigated systems satisfy this condition. Then, on the basis of both the rheological results obtained with the PVA–borate HVPDs and the test already carried out, the efficacy of these aqueous systems as cleaning tools was tested on a surface of a wall painting. The experimentation was made in cooperation with the restorer Barbara Ferriani on a portion of the *Giudizio Universale* (Fig. 8A), a fresco by Carlo Carrà (1881–1966) in the *Palazzo di Giustizia* in Milan. The painted surface had been altered by a uniform thin dark grey layer present all over the surface and constituted by carbonaceous particles mainly derived from atmospheric pollution (Fig. 8B). For the realisation of the paint Carrà used substances highly sensitive to aqueous media like gypsum and white egg as the binding medium, in order to obtain the effect of different colour saturations. The first attempt for the removal of the surface dirt layer showed that deionised water was able to solubilise the surface dark layer but its penetration into the mortar's porous structure caused the swelling of the binder with consequent local surface whitening. In order to avoid all these drawbacks, the cleaning was carried out by means of the 75PVA–borax–H_2O based HVPDs (cleaning tests were performed by means of the systems containing the 7 wt% of 75PVA): according to the Washburn equation, due to their high viscosity, the penetration of the water into the porous support was minimised. The system was applied with a spatula and maintained in contact with the surface for 4 min; thanks to its elasticity, the gel was completely removed in one step without residues left on the painting surface. After the gel application some dark layers were still present on the surface and were completely removed with a second application of the gel (Fig. 8C). It is worth noting that an important advantage in using these gel-like systems, beside the lack of residues, is

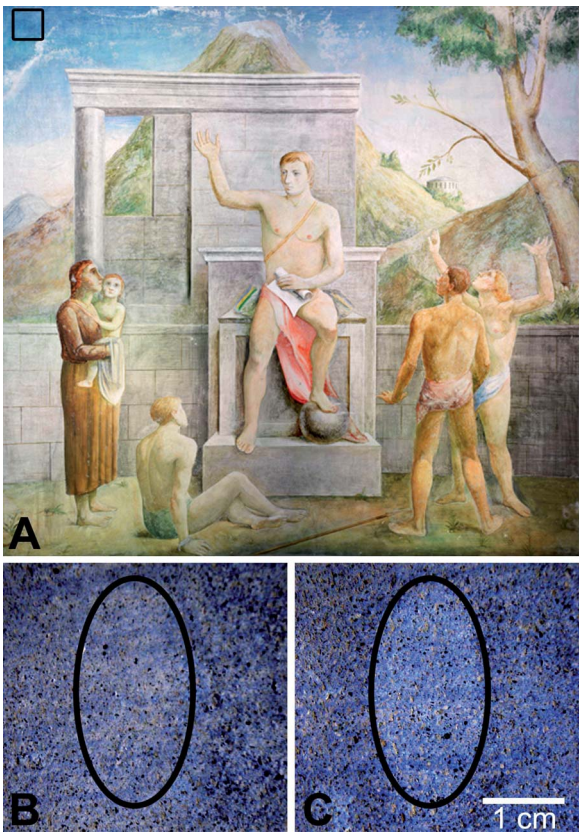

Fig. 8 (A) "*Giudizio Universale*" a XX century wall painting by Carlo Carrà (1881–1966), Palazzo di Giustizia, Milano, Italy. The black box indicates the region where the cleaning test was carried out by means of the 75PVA–borax based HVPD. Magnification of the area interested by the cleaning test before (B) and after (C) the application of the HVPD. The application procedure is described in the Materials and methods section.

related to the selective, controllable and progressive cleaning of the surface.

Conclusions

In this paper 75PVA–borax cross-linked based HVPDs were studied in order to obtain information about the role of the hydrolysis degree, the molecular weight and the concentration in the structural and dynamic properties of the polymer systems; the ratio between the borax and the OH groups of the 75PVA molecules ($OH/B(OH)_4^-$) was maintained equal to 20.4.

Dynamic rheological measurements were also performed in the linear viscoelastic regime for 75PVA concentrations above the entanglement threshold C^*. The frequency sweep indicates that at low 75PVA concentrations, the HVPDs show a behaviour typical of the viscoelastic solutions: in the low frequency regime $G' \sim \omega^2$ and $G'' \sim \omega$. The fitting, carried out by means of a single-mode Maxwell element model, indicated a deviation from this behaviour. The increase of the R^2 value with the 75PVA concentration suggested a multimodal relaxation process. The relaxation spectra calculated from the frequency sweep curves were all characterised by the presence of a single peak whose shape resulted unvaried by increasing the polymer concentration. This indicates that the main relaxation mechanism is independent of the above mentioned parameters. Nevertheless, the increase of the width of the peak observed by increasing the 75PVA concentration could be related to extra relaxation modes, mainly attributable to the enhancement of the entanglement density. Furthermore, it was found that the mean relaxation time τ_H was related to the 75PVA concentration by a power law $\tau_H \sim C^a$ with $1.7 < a < 2.3$. As described by Rubinstein *et al.*,[42] this behaviour indicates that the relaxation is characterised by a sticky reptation mechanism and that the polymer coil is in a 'good' solvent (H_2O) for the 75PVA–borax network, as determined by SAXS analysis. Finally, this paper, together with a recent research[28,45] confirms that, even in the field of the material chemistry applied to the conservation of artefacts, a perfect control of the physico-chemical properties allows an optimisation of the applicative performances.

Acknowledgements

Financial support from the University of Florence Fondi d'Ateneo ex-60% and from the Consorzio interuniversitario per lo sviluppo dei Sistemi a Grande Interfase (CSGI), Florence, Italy, is gratefully acknowledged. Financial support from the Tuscany Region, Italy, SICAMOR Project PAR-FAS is also acknowledged. This work was also partly supported by the European Union, Project NANOFORART (FP7-ENV-NMP-2011/282816).

Notes and references

1 B. Ding, H. Kim, S. Lee, C. Shao, D. Lee, S. Park, G. Kwag and K. Choi, *J. Polym. Sci., Part B: Polym. Phys.*, 2002, **40**, 1261.
2 S. H. Imam, L. Mao, L. Chen and R. V. Greene, *Starch*, 1999, **51**, 225.
3 J. Zeng, A. Aigner, F. Czubayko, T. Kissel, J. H. Wendorff and A. Greiner, *Biomacromolecules*, 2005, **6**, 1484.
4 T. H. Young, N. K. Yao, R. F. Chang and L. W. Chen, *Biomaterials*, 1996, **17**, 2139.
5 T. H. Young, W. Y. Chuang, N. K. Yao and L. W. Chen, *J. Biomed. Mater. Res.*, 1998, **40**, 385.
6 K. Inoue, T. Fujisato, Y. J. Gu, K. Burczak, S. Sumi, M. Kogire, T. Tobe, K. Uchida, I. Nakai, S. Maetani and Y. Ikada, *Pancreas*, 1992, **7**, 562.
7 W. Paul and C. P. Sharma, *J. Biomater. Sci., Polym. Ed.*, 1997, **8**, 755.
8 Y. Hara, S. Kamiya, K. Nishioka, M. Saishin, S. Nakao and A. Yamauchi, *Acta Soc. Ophthalmol. Jpn.*, 1979, **83**, 1478.
9 K. Burczak, E. Gamian and A. Kochman, *Biomaterials*, 1996, **17**, 2351.
10 H. Gao, R. Yang, J. He and L. Yang, *J. Appl. Polym. Sci.*, 2010, **116**, 1459.
11 W. S. Lyoo, S. J. Lee and J. H. Kim, *J. Appl. Polym. Sci.*, 2004, **93**, 1638.
12 J. H. Choi, S. W. Ko, B. C. Kim, J. Blackwell and W. S. Lyoo, *Macromolecules*, 2001, **34**, 2964.
13 R. K. Schultz and R. R. Myers, *Macromolecules*, 1969, **2**, 281.

14 E. V. Basiuk, A. Anis, S. Bandyopadhyay, E. Alvarez-Zauco, S. L. I. Chan and V. A. Basiuk, *Superlattices Microstruct.*, 2009, **46**, 937.
15 A. L. Kjøniksen and B. Nyström, *Macromolecules*, 1996, **29**, 5215.
16 L. V. Angelova, P. Terech, I. Natali, L. Dei, E. Carretti and R. G. Weiss, *Langmuir*, 2011, **27**, 11671.
17 C. Y. Chen, J. Y. Guo, T. L. Yu and S. C. Wu, *J. Polym. Res.*, 1998, **5**, 67.
18 S. J. Kim, C. K. Lee and S. I. Kim, *J. Appl. Polym. Sci.*, 2004, **92**, 1467.
19 K. Nakamura, T. Hatakeyama and H. Hatakeyama, *Polymer*, 1983, **24**, 871.
20 Y. Sakai, S. Kuroki and M. Satoh, *Langmuir*, 2008, **24**, 6981.
21 W. Goodwin and R. W. Hughes, *Rheology for Chemists: an introduction*, Royal Society of Chemistry, Cambridge, 2000.
22 H. A. Barnes, J. F. Hutton and K. Walters, *An Introduction to Rheology*, Elsevier, Amsterdam, 1989.
23 N. Nemoto, *Macromolecules*, 1999, **32**, 8872.
24 P. D. Hong, C. M. Chou and H. T. Huang, *Eur. Polym. J.*, 2000, **36**, 2193.
25 E. Carretti, S. Grassi, M. Cossalter, I. Natali, G. Caminati, R. G. Weiss, P. Baglioni and L. Dei, *Langmuir*, 2009, **25**, 8656.
26 E. Carretti, I. Natali, C. Matarrese, P. Bracco, R. G. Weiss, P. Baglioni and L. Dei, *J. Cult. Herit.*, 2010, **11**, 373.
27 E. Carretti, M. Bonini, L. Dei, B. H. Berrie, L. V. Angelova, P. Baglioni1 and R. G. Weiss, *Acc. Chem. Res.*, 2010, **43**, 751.
28 J. Domingues, N. Bonelli, R. Giorgi, E. Fratini, F. Gorel and P. Baglioni, *Langmuir*, 2013, **29**, 2746.
29 I. Natali, E. Carretti, L. Angelova, P. Baglioni, R. G. Weiss and L. Dei, *Langmuir*, 2011, **27**, 13226.
30 A. A. Sobczuk, S. Tamaru and S. Shinkai, *Chem. Commun.*, 2011, **47**, 3093.
31 T. N. Blanton, M. Rajeswaran, P. W. Stephens, D. R. Whitcomb, S. T. Misture and J. A. Kaduk, *Powder Diffr.*, 2011, **26**, 313.
32 M. Shibukawa, K. Aoyagi, R. Sakamoto and K. Oguma, *J. Chromatogr., A*, 1999, **832**, 17.
33 D. J. Abdallah, L. Lu and R. G. Weiss, *Chem. Mater.*, 1999, **11**, 2907.
34 T. Seo, S. Take, K. Miwa, J. K. Hamada and T. Iijimar, *Macromolecules*, 1991, **24**, 4255.
35 T. Kanaya, N. Takahashi, K. Nishida, H. Seto, M. Nagao and Y. Takeba, *Phys. B*, 2006, **385–386**, 676.
36 A. L. Kjoniksen and B. Nystrom, *Macromolecules*, 1996, **29**, 5215.
37 F. Horkay and B. Hammouda, *Colloid Polym. Sci.*, 2008, **286**, 611.
38 P. G. De Gennes, *Scaling concepts in polymer physics*, Cornell University Press, Ithaca, New York, 1979.
39 B. A. Schubert, E. W. Kaler and N. J. Wagner, *Langmuir*, 2003, **19**, 4079.
40 J. Honerkamp and J. Weese, *Rheol. Acta*, 1993, **32**, 65.
41 M. Doi and S. F. Edwards, *J. Chem. Soc., Faraday Trans.*, 1978, **74**, 1818.
42 M. Rubinstein and A. N. Semenov, *Macromolecules*, 2001, **34**, 1058.
43 H. Hatakeyama and T. Hatakeyama, *Thermochim. Acta*, 1998, **308**, 3.
44 P. Baglioni, D. Berti, M. Bonini, E. Carretti, L. Dei, E. Fratini and R. Giorgi, *Adv. Colloid Interface Sci.*, 2014, **205**, 361.
45 I. Natali, P. Tempesti, E. Carretti, M. Potenza, S. Sansoni, P. Baglioni and L. Dei, *Langmuir*, 2014, **30**, 660.

